Evidence that a single mechanism drives the finite-temperature phase transition in full QCD

H. Gausterer
Institut für Theoretische Physik der Universität Graz, A-8010 Graz, Austria

J. Potvin
Physics Department, Boston University, Boston, Massachusetts 02215
and Department of Mathematics, Statistics, and Computer Science, Dalhousie University, Halifax, Nova Scotia, Canada B3H 3J5

S. Sanielevici
Supercomputer Computations Research Institute, Florida State University, Tallahassee, Florida 32306
(Received 4 January 1990)

We simulate finite-temperature QCD with two flavors of dynamical staggered quarks on a $10^3\times 4$ lattice. Along with the real part of the Polyakov loop and with the chiral condensate, we monitor the behavior of the topological charge across the phase transition. For two different values of the quark mass ($ma=0.2$, $ma=0.025$) we find good evidence that these observables are equivalent characteristics of the phase in which the theory finds itself. However, the phase transition is clearly steeper for $ma=0.025$. Some implications of these results are discussed.

I. INTRODUCTION

Full quantum chromodynamics (QCD) with general values of the quark mass m and of the number of degenerate quark flavors n_f is not characterized by any easily computable order parameters which would label its phases at finite temperature. As a consequence, our physical understanding of its phase structure has been mainly guided by extrapolations from two special limits where such order parameters have been defined. Indeed, knowledge of these order parameters enables one to construct effective theories of the phase transition.[1-3] However, extrapolations from these limits to the general theory cannot be justified *a priori*.

On the other hand, several models based on assumptions about general properties of full QCD have been put forward over the years. Among these, models of the topological structure of color field configurations[4-6] are especially interesting, since they have the potential to make contact with the effective theories while simultaneously solving the $U_A(1)$ problem of zero-temperature hadron spectroscopy.[7,8] Unfortunately, the approximations used to make these models calculable are less systematic than those which define the effective theories based on the existence of order parameters.

Recently, a series of lattice simulations of full QCD at finite temperature has advanced our knowledge of its phase diagram.[9,10] As is well known, lattice simulations work directly on the level of the QCD Lagrangian; the approximations one uses to make them numerically calculable with a given amount of computing resources can be relaxed systematically as the resources grow. Such simulations do not explore the phase diagram by focusing on assumptions about dominant dynamical mechanisms, they simply measure lattice averages of observables such as the Polyakov loop and the chiral condensate. Recent progress has also made it possible to measure the topological susceptibility on the lattice.[11-16] Thus, it becomes feasible to use lattice simulations to analyze issues which have been central to the models in Refs. 2–6, such as the dependence of the topological content of QCD field configurations on m, n_f, T and its relation to deconfinement and chiral-symmetry breaking. In this paper, we use lattice simulations of full QCD to compare the temperature dependence of the topological susceptibility to that of the observables which become order parameters in the quenched and chiral limits of the theory.

Let us begin by discussing the physical motivation for such a study in greater detail. In the quenched limit ($m\rightarrow\infty$ or $n_f\rightarrow 0$), the dynamics of QCD reduces to that of pure SU(3) theory. The phases of the latter can be described in terms of the confinement order parameter $\langle L\rangle$ (the average Polyakov loop, a complex number). Effective models of its finite-temperature phase transition can be constructed on this basis.[1] At subcritical temperatures $T<T_c$, the theory is in its Z_3 symmetric, confined phase, where the only physical degrees of freedom are glueballs. For $T>T_c$, Z_3 symmetry is broken so free gluons can exist (deconfinement).

Starting from this picture, one may consider the consequences of allowing dynamical quarks as a perturbation.[17] While Z_3 symmetry is always broken in the presence of dynamical quarks, the real part of the Polyakov loop, $\langle \mathrm{Re}L\rangle$, still differentiates between two phases: it is small (but nonzero) at low temperatures, while becoming large at sufficiently high temperatures. Given the phenomenological fact of color confinement at zero temperature, one interprets the low-T phase as the hadronic phase of QCD. The phase transition is still interpreted as a deconfinement transition, as in the quenched limit.

Therefore one expects that free quarks and gluons can exist in the high-T phase, which is labeled the "plasma phase of QCD" for this reason.

In the limit $m \to 0$, the QCD Lagrangian is characterized by exact chiral symmetry. The corresponding order parameter is the quark condensate $\langle \bar{\psi}\psi \rangle$. Therefore, one can construct an effective model of the finite-temperature behavior of QCD in this limit.[2] This model exhibits a low-T phase where $\langle \bar{\psi}\psi \rangle \neq 0$ and a high-T phase where the order parameter is zero. Since the physical u and d current-quark masses are small, one expects that the real world can be reached by a small perturbation of this chiral limit. While $\langle \bar{\psi}\psi \rangle$ will not remain an order parameter, being always nonzero, it will still be sensitive to the dynamical breaking of (approximate) chiral symmetry. Now, hadron spectroscopy implies that chiral symmetry is dynamically broken in the zero-temperature theory. The effective model thus predicts a finite-temperature transition to a phase where chiral symmetry cannot be dynamically broken. It is tempting to identify the low-T phase with the hadronic phase of the quenched paradigm, and the chirally symmetric high-T phase with the plasma phase. However, the effective-model approach cannot warrant this identification, since the notion of confinement is only defined close to the quenched limit. Such an identification requires some unifying dynamics from which both effective theories should emerge in the appropriate limits.

The topology-based models of the QCD vacuum[4-6] seem to offer such a unifying framework. In such models, topological properties can simultaneously explain confinement and chiral-symmetry breaking at zero temperature, as well as the loss of these properties in the QCD phase transition. For example, Ref. 4 suggests that deconfinement could be caused by the suppression of topological susceptibility as temperature increases: in an instanton-gas model of the SU(3) vacuum, the string tension can be shown to be finite for low temperature and to undergo a sharp transition to a phase where it is zero. This is brought about solely by the decrease of the instanton-gas density as the temperature grows. On the other hand, chiral-symmetry breaking at zero temperature can also be explained in topological terms.[5,6] Essentially, the QCD vacuum in the massless limit is dominated by instanton–anti-instanton pairs whose interactions break chiral symmetry. As their numbers are reduced with the increase of temperature, the chiral-symmetry-breaking effect of instanton–anti-instanton pairs can also be expected to disappear.

In addition, topology-based models are designed to incorporate the breaking of $U_A(1)$ symmetry at zero temperature, and they predict its restoration as temperature increases. It is interesting that in the framework of the effective theory of Refs. 2, the order of the chiral-restoration transition depends on the details of $U_A(1)$-symmetry restoration.

Such models would therefore predict a close relationship between the temperature dependences of the topological susceptibility, the Polyakov loop and the chiral condensate. This prediction can be checked in a lattice simulation. Furthermore, we now know[10] that the behavior of the full theory close to the phase transition depends markedly on m and n_f. In the topology-driven single-mechanism scenario one would then expect that the susceptibility and all the other phase characteristics should react in unison to changes in (m,n_f). This too can be checked by numerical simulations.

In the present paper we report the results of such an investigation. Section II discusses the role of topological charge in full QCD. Section III describes the way we have measured it on the lattice, and other details of the simulation. Our results on the relationship between the topological susceptibility and other phase characteristics are presented in Sec. IV. Some comments on the significance of these results are made in Sec. V.

II. TOPOLOGICAL CHARGE IN FULL QCD

Let $\{A_\mu(x_\mu), \psi^k(x_\mu), \bar{\psi}^k(x_\mu)\}$ denote a configuration of full continuum QCD (k counts quark flavors and color indices have been omitted). Since the quarks are dynamical, the gluon field tensor $F_{\mu\nu}(x_\mu)$ and its dual $\tilde{F}_{\mu\nu}$ will be different from what they would have been in pure SU(3) theory at the same color coupling. Therefore, even though the topological charge is defined by the same formula as in the pure Yang-Mills case,

$$Q = \frac{1}{32\pi^2} \int_0^{1/T} dt \int d^3x \, \mathrm{Tr}(F_{\mu\nu}\tilde{F}_{\mu\nu}) , \tag{1}$$

it does reflect the quark dynamics as well. Note that Eq. (1) has been written for the finite-temperature theory: the fields are defined on a slab of space-time, of volume V, whose timelike extension is given by the inverse temperature. $A_\mu(x_\mu)$ is periodic in the time direction, while the quark and antiquark fields are antiperiodic.

Since Q includes the effects of quark dynamics, the topological classification[4] of smooth, periodic, finite-energy field configurations is applicable to full QCD. Restricting oneself to such configurations, one can write

$$Q = N + \sum_\alpha q_\alpha \ln\lambda_\alpha / 2\pi i . \tag{2}$$

Here λ_α are the eigenvalues of the Polyakov loop operator $L(\mathbf{x})$ at spatial infinity, q_α are quantized magnetic charges, and the integer N is the Pontryagin index.

Reference 4 goes on to prove the following statements for asymptotically high temperatures.

(i) Noninteger values of Q are suppressed; instantons are the dominant topological objects. This is essentially because, for high temperatures, only configurations which have $L(\infty)=1$ (the maximum value of the Polyakov loop) contribute to $Z[A_\mu, \psi^k, \bar{\psi}^k]$. Therefore the sum in Eq. (2) vanishes.

(ii) Spatially large instantons are suppressed, and the instanton density decreases with temperature. Thus, at asymptotic temperatures, the QCD vacuum can be described by a dilute gas of noninteracting instantons.

As opposed to the above properties, the relationship between the topological susceptibility and the $U_A(1)$ problem at zero temperature has only been proven in the quenched approximation. The Witten-Veneziano formula, which is true for full QCD (see Refs. 8 and 16), introduces a special glue-glue correlation function $C(T=0)$:

$$2n_f(f_s^2 m_s^2 - f_\pi^2 m_\pi^2) = -C(0) \quad (3)$$

(the subscript s indicates the pseudoscalar flavor singlet, such as the η' in the real world). In the quenched approximation, it can be shown[7,8] that $C(0)$ is given by the topological susceptibility of *pure* SU(3) theory. In full QCD, the susceptibility continues to act as the "core" of $C(0)$ [$C(0)=0$ by definition if the susceptibility vanishes]. However, in full QCD, the susceptibility contains additional pseudoscalar pole terms which must be removed to get $C(0)$. This calculation has not been done except in a special approximation[7] which requires, among other things, that the quark masses be infinitesimal. In this approximation, one simply has

$$C(0) = 4n_f^2\chi - 2n_f f_s^2 m_s^2 \quad (4)$$

($\chi = \langle Q^2 \rangle / V$ denotes the topological susceptibility of full QCD).

A relationship between topological properties and chiral symmetry has been formulated in the chiral limit at zero temperature.[5] Configurations with $Q \neq 0$ do not contribute to $Z[A_\mu, \psi^k, \bar\psi^k]$ if any of the quark fields are massless. Therefore, $\lim_{m\to 0}\chi(T=0)=0$. At zero temperature, it is not clear that instantons and anti-instantons are the dominant topological objects in the vacuum [see property (i) above]. In any case, topological objects must form neutral aggregates. Taking these to be instanton–anti-instanton pairs, one can show that they interact by exchanging pairs of massless quarks and antiquarks.[5,6] This interaction breaks chiral symmetry if the gauge coupling becomes strong enough. It also follows that the $T=0$ vacuum cannot be an ideal gas such as the dilute instanton gas which should exist at asymptotically high temperature.[6]

From Eqs. (3) and (4) it follows that, for sufficiently small quark masses,

$$\chi = f_\pi^2 m_\pi^2 / 2n_f = \frac{m}{2}\langle \bar\psi\psi \rangle \ , \quad (5)$$

where the last equality results from current algebra.[18] It has not been demonstrated that Eq. (5) actually applies to the real world: the true shape of the function $\chi(m)$ has not been mapped out yet.[16] We only know that it interpolates between the chiral limit Eq. (5) and the quenched limit $\lim_{m\to\infty}\chi(T=0)=C(0)$, which we discussed above.[19]

The symmetry of the effective model of the finite-temperature chiral-restoration transition[2] allows for the presence of an $U_A(1)$-breaking term whose strength is given by a temperature-dependent function $C(T)$. For $n_f=2$, the chiral-restoration transition is first order if and only if $C(T_c) \ll C(0)$. If one could generalize the equality between the quenched susceptibility and $C(0)$ to finite temperature, the suppression of χ as $T\to\infty$ [by asymptotic property (ii) above] would indicate that such an inequality is indeed possible in QCD. To actually prove this inequality, one would then have to display the T dependence of the quenched χ explicitly [and to know $T_c(m,n_f)$ in physical units].

In summary, there are many tantalizing hints that topological susceptibility might provide a link between the Polyakov loop [see Eq. (2)], the chiral condensate [see Eq. (5)], and the $U_A(1)$-symmetry-breaking parameter C. Analytic proofs of these relationships have only been given, however, for special combinations of (m,n_f,T). It seems interesting to use lattice simulations to see if these observables are indeed correlated in the interior of the phase diagram.

III. THE SIMULATION

The temperature dependence of the topological susceptibility in pure SU(3) theory has been studied on the lattice in Refs. 14 and 15. It appears that χ undergoes a sharp ("discontinuous") suppression at the deconfinement temperature T_D. The considerations in Sec. II lead us to study χ and its correlation with $\langle \mathrm{Re}L \rangle$ and $\langle \bar\psi\psi \rangle$, in the phase transition region of full QCD with various (m,n_f). In particular, we set $n_f=2$ and we use two values of the quark mass for which previous numerical studies[10] have found very different behavior of $\langle \mathrm{Re}L \rangle$ and $\langle \bar\psi\psi \rangle$ across the phase transition.

We generated our full QCD configurations by means of a second-order Langevin algorithm.[20] The lattice size was $10^3\times 4$; the quark masses were $ma=0.2$ and $ma=0.025$. We used a Langevin step size of $\epsilon=0.01$, for which previous experience shows that the systematic error of our second-order algorithm is negligible for $ma=0.2$, and small for $ma=0.025$. The fermion matrix inversions required for updating were performed using a conjugate-gradient algorithm. The stopping requirement was that an average element of the residue vector would be less than $\frac{2}{3}\times 10^{-4}$.

For both values of the quark mass, we generated configurations in the phase transition region. For $ma=0.2$, we used the following values of β: 5.36, 5.40, 5.42, 5.44, 5.46, 5.48, 5.52. For $ma=0.025$, we ran at $\beta=5.28$, 5.30, 5.34. In all cases, configurations were grown from a hot (random) start. Measurements of the observables to be monitored in this study were begun once the Wilson loops up to 2×2 and the real and imaginary parts of $\langle L \rangle$ indicated that equilibrium had been reached. Configurations were kept for measurement every 250 iterations (for $ma=0.2$), respectively, every 200 iterations for $ma=0.025$.

On each configuration retained for analysis, we began by measuring $\langle \mathrm{Re}L \rangle$. The chiral condensate was computed using five random vectors.[21] The required fermion matrix inversions were performed with the same conjugate-gradient algorithm and using the same stopping criterion that was employed for updating. We also recorded the number of conjugate-gradient iterations required to reach the prescribed residue, for each of the five inversions. We used the arithmetic mean of these iteration numbers as another characteristic of the configuration in question. This number will be denoted by NCG in Sec. IV.

In order to extract the total topological charge of the configuration, we have used the relaxation (cooling) algorithm described in Ref. 16. The given configuration is subjected to a noiseless Langevin equation with a pure SU(3) driving force, discretized to first order in the step size δ. We use the pure gauge action and not the effective action of the full theory, because we are interested in finding (approximate) solutions to the Yang-Mills self-duality conditions. Experience shows that a diffusion step size of $\delta=0.1$ is optimal.

After every cooling step, we measure the quantity

$$Q_L = \frac{1}{32\pi^2}\epsilon_{\mu\nu\rho\sigma}\sum_x \mathrm{Re\,Tr}P^{\mu\nu}(x)P^{\rho\sigma}(x) , \qquad (6)$$

where $P^{\mu\nu}(x)$ is the plaquette formed by the links which emanate from lattice site x in the directions μ,ν. The space-time distribution of this quantity is monitored at each cooling step, by keeping track of the locations of the minimum and maximum of its density and of the ratio of the maximum density to the total Q_L. A typical cooling run is shown in Fig. 1.

For any finite lattice spacing a, the lattice estimator Eq. (6) differs from the continuum charge Q by ultraviolet fluctuations.[22] Q_L gets contributions not only from physical topological objects, but also from lattice artifacts. The latter are generally localized objects whose size is of the order of one lattice spacing, while the objects which survive the continuum limit are much broader. Cooling algorithms are designed to eliminate these artifacts.[13,14] By cooling, spatially extended topological objects are gradually "squeezed" out of the lattice. The small objects, such as the artifacts, are squeezed out first; the broadest objects disappear last. Plateaus in the cooling history indicate approximate solutions of the self-duality equations.[14] For example, one would interpret the last plateau in Fig. 1 as being due to an anti-instanton. The smaller first plateau could be due to the presence of another, smaller, anti-instanton which gets smoothed out around cooling iteration 130. (The total charge along this first plateau should be -2 in the continuum; one might attribute the fact that here it appears to be -1.5 to

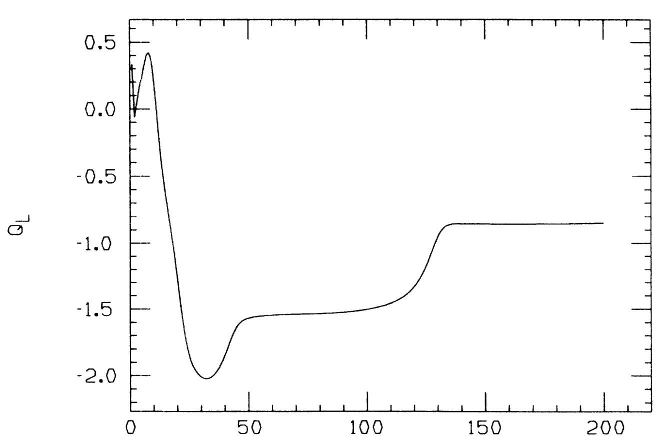

FIG. 1. A typical cooling history (relaxation step size $\delta=0.1$).

the effects of the rather large lattice spacing.) On the other hand, the smaller object may also have been a lattice artifact.

Thus, such interpretations are not entirely trustworthy. A clear separation between the size scales of true topological objects, on one hand, and of lattice artifacts, on another, only exists if the configuration to be analyzed has been obtained sufficiently close to the continuum limit to begin with.[14] Our configurations were taken at rather strong couplings, so it is not clear if relaxation does not eliminate genuine topological objects along with the artifacts. In Fig. 1, it is not even clear if the (negative) peak reached after about 30 iterations is due to a genuine topological object or not.

In view of these difficulties, which essentially mean that assigning a topological charge to a configuration on the basis of a cooling history such as Fig. 1 is a subjective exercise, we have taken the following approach. For each configuration, we record both the largest assignable value of $|Q_L|$ (such as $|Q_L^>|=2.02$ in Fig. 1) and its lowest assignable value ($|Q_L^<|=0.85$ in the case of Fig. 1). We do not attempt to round off these charges to integers; if the charge is indeed quantized, this should become apparent when an ensemble of configurations is analyzed.[16]

IV. RESULTS

In Fig. 2 we show the temperature dependences of our results for the nontopological observables $\langle\bar{\psi}\psi\rangle$, *NCG*, and $\langle \mathrm{Re}L \rangle$. In order to compare the results for the two values of the quark mass, we have converted β into temperature T using two-loop scaling. We find $\beta_c=5.46$ for $ma=0.2$ and $\beta_c=5.30$ for $ma=0.025$; the ordinates in Figs. 2 are obtained by converting these critical couplings into critical temperatures and forming the ratios T/T_c. The effects of two-loop scaling violations should be reduced by this procedure of forming dimensionless ratios.[21] In any case, the qualitative comparisons which are made possible by this procedure convey two important points. First, they reveal the relationships between these observables and temperature, which will serve as a reference for Figs. 3–5. Second, we see that the phase transition, as expressed by the behavior of $\langle\bar{\psi}\psi\rangle$ and *NCG*, is much steeper for $ma=0.025$ than for $ma=0.2$. In fact, based on *NCG* it is questionable whether there is a transition for $ma=0.2$ at all. $\langle \mathrm{Re}L \rangle$ is much less sensitive to the change in the quark mass. This is consistent with the "chiral" character of the QCD transition at low quark masses:[9,10] by definition, both $\langle\bar{\psi}\psi\rangle$ and *NCG* reflect the eigenvalue structure of the staggered fermion matrix.

Figures 3 show the cross correlations between these nontopological phase characteristics. Each point in these plots represents a configuration; we have collected all the measurements taken at all temperatures. The relationships between *NCG* and $\langle \mathrm{Re}L \rangle$ are essentially the mirror images of Figs. 3(a) and 3(b) and need not be shown here.

Figures 4 plot the absolute values of Q_L measured on all configurations we have analyzed, against the values of $\langle\bar{\psi}\psi\rangle$ measured on those same configurations. Figures 4(a) and 4(c) show the highest (peak) assignable values; Figs. 4(b) and 4(d) show the lowest assignable values

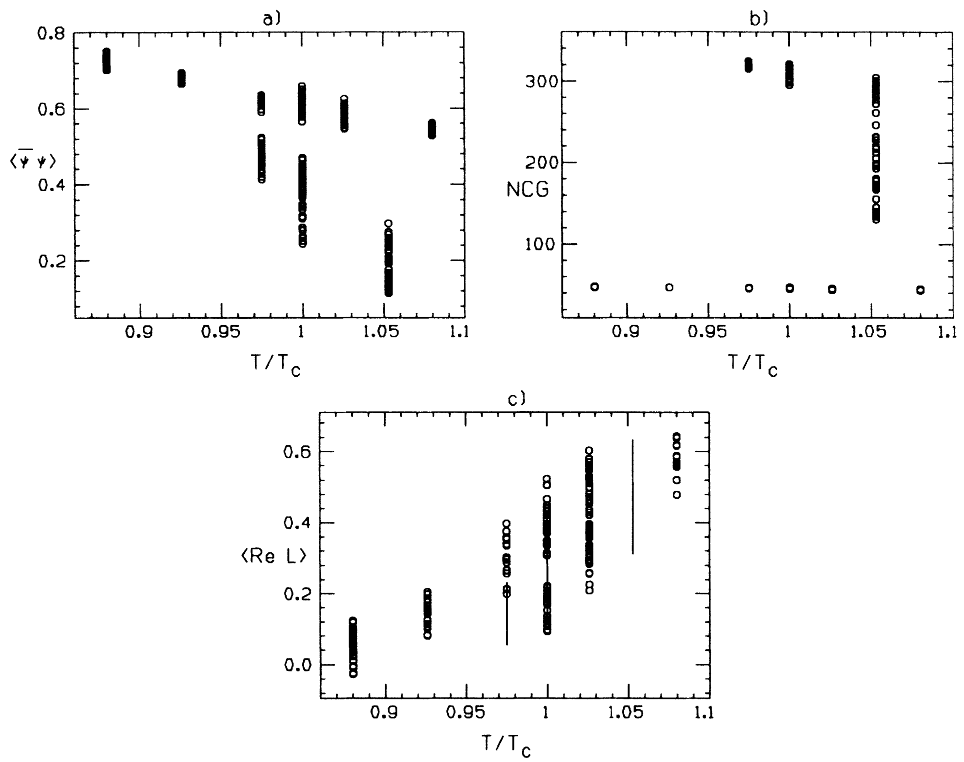

FIG. 2. The dependence of nontopological observables on the relative temperature. (a) The abscissa is the temperature normalized to the critical temperature, as described in the text. The ordinate is the chiral condensate. Results for $ma=0.2$ are consistently larger than those for $ma=0.025$. (b) Same as in (a), but for the average number of conjugate-gradient iterations. Here the results for $ma=0.025$ are always higher than those for $ma=0.2$. (c) Same as in (a), but for $\langle \mathrm{Re}L \rangle$. The results for $ma=0.2$ are indicated as open circles and those for $ma=0.025$ as vertical bars.

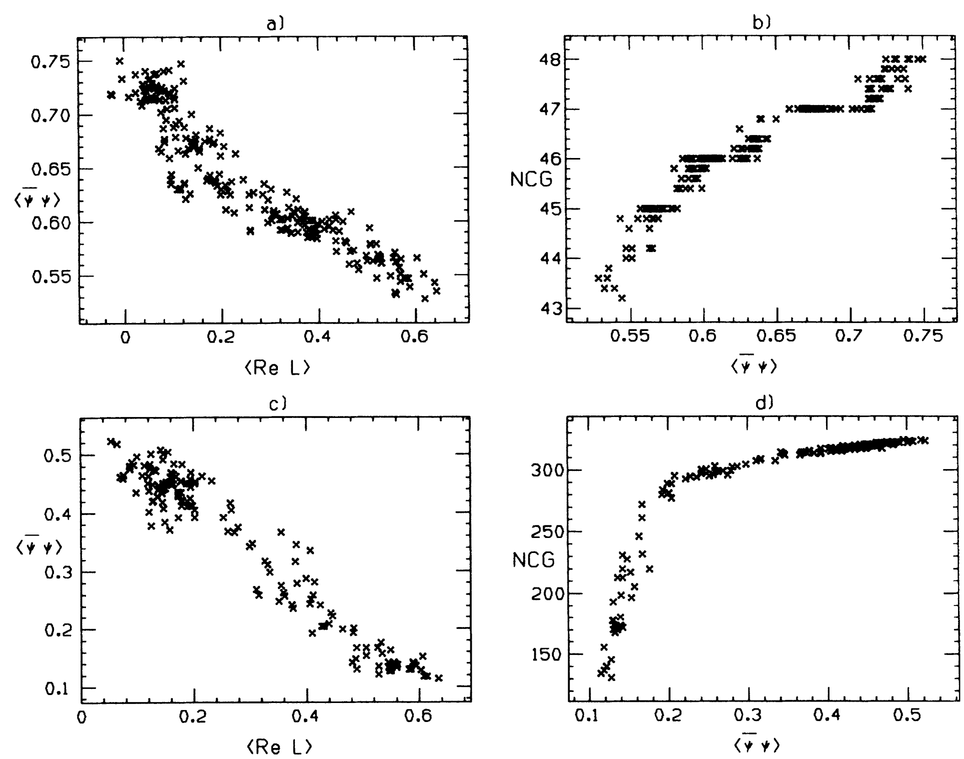

FIG. 3. Correlations between nontopological observables, measured on all configurations taken at all temperatures. (a) $ma=0.2$: $\langle \bar{\psi}\psi \rangle$ vs $\langle \mathrm{Re}L \rangle$. (b) $ma=0.2$: *NCG*, the average number of conjugate-gradient iterations needed to invert the staggered fermion matrix to a specified precision, vs $\langle \bar{\psi}\psi \rangle$. (c) Same as (a), but for $ma=0.025$. (d) Same as (b), but for $ma=0.025$.

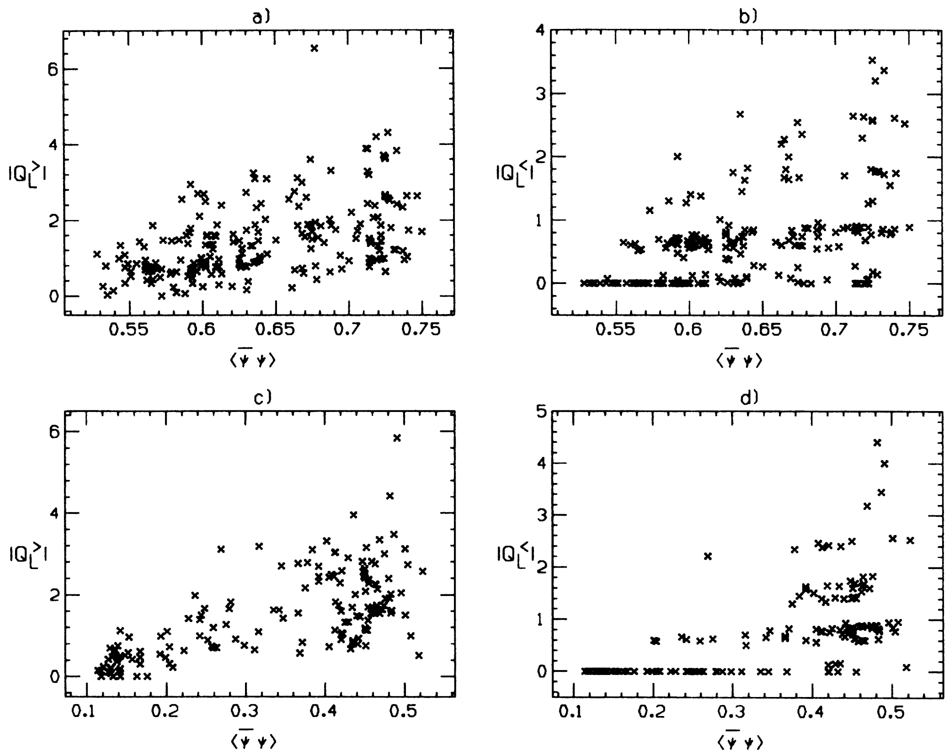

FIG. 4. Correlations between the topological charge and the quark condensate, measured on all configurations taken at all temperatures. (a) $|Q_L^>|$, the absolute value of Q_L as extracted by the peak method, vs $\langle\bar{\psi}\psi\rangle$, for $ma=0.2$. (b) Same as (a), but for $|Q_L^<|$, the absolute value of Q_L as extracted by the lowest-plateau method. (c) Same as (a), but for $ma=0.025$. (d) Same as (b), but for $ma=0.025$.

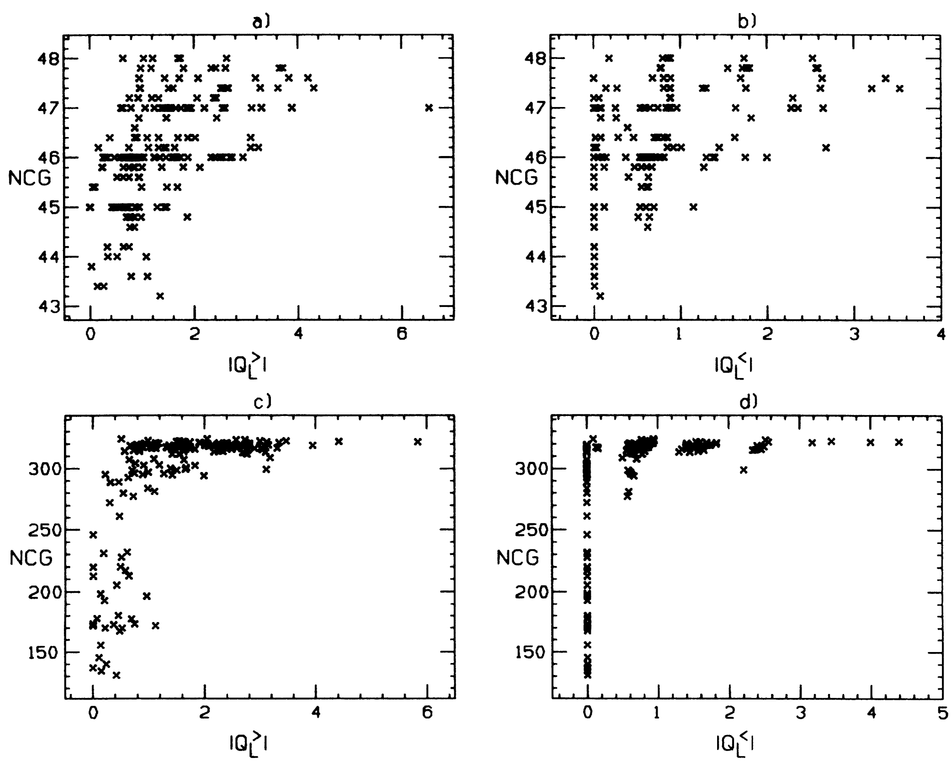

FIG. 5. Correlations between the topological charge and the average number of conjugate-gradient iterations, measured on all configurations taken at all temperatures. (a) *NCG* vs $|Q_L^>|$, for $ma=0.2$. (b) *NCG* vs $|Q_L^<|$, for $ma=0.2$. (c) Same as (a), but for $ma=0.025$. (d) Same as (b), but for $ma=0.025$.

(measured on the last plateau in the cooling history). Quantization is obvious for the low values and seems to be absent for the high values. For both methods of charge assignment, however, there is a clear correlation with the quark condensate. In all these scatter plots, there is evidence of two phases. In the high-temperature phase, $\langle \bar{\psi}\psi \rangle$ is small [see Fig. 2(a)] and the occurrence of configurations with large $|Q_L|$ is unlikely. In the low-temperature phase, $\langle \bar{\psi}\psi \rangle$ is larger; the distribution of $|Q_L|$ is centered around nonzero charge and configurations with large $|Q_L|$ occur. Comparing the two quark masses, the ranges of $|Q_L|$ are quite similar. The ranges of $\langle \bar{\psi}\psi \rangle$, on the other hand, are very different, reflecting the situation in Fig. 2.

The relationships between topological charge and $\langle \mathrm{Re}L \rangle$ are again found to be essentially mirror images of Figs. 4 and thus contain no new information. On the other hand, Fig. 3(d) suggests that *NCG* is a very interesting and sensitive phase characteristic. For this reason we show, in Figs. 5, the correlations between the topological charge and *NCG*. These are similar to Figs. 4, but they seem to bring out the essentials in a more poignant way.

V. DISCUSSION

Our results suggest that all the observables we studied above are equivalent characteristics of the phase in which full QCD finds itself at a given temperature. In particular, the topological susceptibility in full QCD with light dynamical quarks is seen to be suppressed in the high-temperature phase, just as Refs. 14 and 15 found it to be suppressed in pure SU(3) theory.

While these qualitative numerical results cannot prove the single-mechanism scenario of the QCD phase transition, they are certainly consistent with it. It appears to be appropriate to think in terms of a single QCD phase transition characterized by a set of equivalent observables. This seems to be more natural, in view of our results, than to think in terms of three distinct physical mechanisms [deconfinement, chiral-symmetry restoration, restoration of $\mathrm{U}_A(1)$ symmetry]. We have seen that the steepness of the transition depends on the particular combination of (m,n_f), while the correlations between phase characteristics seem to remain invariant. This suggests that the order of the transition may well vary from one region of the phase diagram to another, while still being due to a single mechanism.

In this context, let us also recall the similarity in the behavior of the baryon-number susceptibilities[21] in low-mass full QCD and in the quenched approximation. This suggests that the essential mechanism behind the transition is the same in both cases, having to do with a change in the eigenvalue spectrum of the fermion matrix. This fits in well with the present results, since $\langle \bar{\psi}\psi \rangle$, *NCG*, and the topological susceptibility all reflect this eigenvalue structure. The specific effects of dynamical quarks upon the eigenvalue structure appear to be responsible for the dependence of the transition on (m,n_f).

At present, we do not have enough statistics to warrant drawing any conclusions based on the temperature dependence of the averages of the observables we have studied. It also seems inappropriate to express the topological susceptibilities in physical units at this stage. The example of pure SU(3) theory teaches us that deciding on the order of the QCD phase transition can be a much more difficult and costly effort than was previously realized.[12] Even if we pushed our statistics much further, we could not conclude reliably on the orders of the phase transitions at $ma=0.2$ and $ma=0.025$, just on the basis of studying a single volume (which, moreover, only has $n_t=4$ time slices and is thus certainly not in the scaling region[23]).

On the other hand, it does seem worthwhile to pursue this study in other directions. One may want to study the function $\chi(T,m)$ within the hadronic phase. In particular, will the susceptibility (in physical units) increase significantly as $T\rightarrow 0$, and how will it be suppressed as $m\rightarrow 0$? Also, one might expand the statistics of our runs at selected temperatures above and below the phase transition and then compare the histograms of $|Q_L|$ to the predictions of various topological models of the QCD vacuum. The data we have so far suggest that the dilute–instanton–anti-instanton–gas approximation (DGA) fails in the hadronic phase, no matter which procedure we use to assign the topological charge of a configuration (see also Ref. 16). It would be interesting to see if the instanton-liquid models of Ref. 6 can do better. Above the phase transition, our present data cannot rule out that the charge distribution extracted by the plateau method is in fact consistent with the DGA. Of course, especially in the high-T phase where nonzero charge is improbable, it will take considerable statistics to check this in detail. The charge extracted by the peak method clearly does not obey the DGA, even in the high-T phase. Again, one might want to confront the measured distribution with the predictions of Ref. 6.

In this context, it is interesting to recall the findings of Refs. 12 and 13. These studies, which have only been performed for SU(2) so far, suggest that the topological excitations which are responsible for confinement are not instantons. It would not be surprising if the same held true for pure SU(3) theory and for full QCD, in view of the fact that instantons are only guaranteed to dominate at asymptotically high temperatures, where confinement is lost.

As we have indicated, there are still some problems associated with the measurement of topological charge on the lattice. We are keeping all the configurations generated in this study, so they will be available for examination by other methods of extracting topological charge.[11] One should also keep in mind that this was a first-generation simulation of QCD with dynamical quarks, done on a single volume with small timelike extension, with an algorithm which is not exact and whose way of emulating two continuum quark species has never been rigorously justified.

ACKNOWLEDGMENTS

J. P. thanks the Nippon Electric Company, the Government of Nova Scotia and the Government of Canada for financial support. S.S. would like to acknowledge the Aspen Center for Physics, where part of this work was done. This work was supported in part by the U.S. Department of Energy under Contract No. DE-FC05-85ER250000. The computations were performed on the Cray-YMP at the Pittsburgh Supercomputer Center, under Grant No. PHR54MP.

[1]B. Svetitsky, Phys. Rep. **132**, 1 (1986).

[2]R. D. Pisarski and F. Wilczek, Phys. Rev. D **29**, 338 (1984); H. Gausterer and S. Sanielevici, Phys. Lett. B **209**, 533 (1988).

[3]H. Goldberg, Phys. Lett. **131B**, 133 (1983); A. Margaritis and A. Patkos, Phys. Lett. B **178**, 272 (1986); A. Barducci, R. Casalbuoni, S. De Curtis, R. Gatto, and G. Pettini, *ibid.* **231**, 463 (1989).

[4]D. Gross, R. D. Pisarski, and L. Yaffe, Rev. Mod. Phys. **53**, 43 (1981).

[5]C. G. Callan, R. Dashen, and D. Gross, Phys. Rev. D **17**, 2717 (1978); **19**, 1826 (1979); D. Caldi, Phys. Rev. Lett. **39**, 121 (1977); R. D. Carlitz and D. B. Creamer, Ann. Phys. (N.Y.) **118**, 429 (1979).

[6]"Instanton liquid" models of the QCD vacuum have been proposed by several authors: see E. V. Shuryak, Nucl. Phys. **B203**, 93 (1982); D. I. Dyakonov and V. Yu. Petrov, *ibid.* **B245**, 259 (1984). The relationship with chiral-symmetry restoration at finite temperature is discussed by I. M. Ilgenfritz and E. V. Shuryak, Nucl. Phys. **B319**, 511 (1989).

[7]G. Veneziano, Nucl. Phys. **B159**, 213 (1979); Phys. Lett. **95B**, 90 (1980).

[8]J. Smit and J. C. Vink, Nucl. Phys. **B284**, 234 (1987); **B298**, 557 (1988).

[9]See, for example, the following review articles: J. Cleymans, R. V. Gavai, and E. Suhonen, Phys. Rep. **130**, 217 (1986); M. Fukugita, in *Field Theory on the Lattice,* proceedings of the International Symposium, Seillac, France, 1987, edited by A. Billoire *et al.* [Nucl. Phys. B (Proc. Supp.) **4**, 105 (1988)]; in *Lattice '88,* proceedings of the International Symposium, Batavia, Illinois, 1988, edited by A. Kronfeld and P. B. Mackenzie [*ibid.* **9**, 291 (1989)]; A. Ukawa, in *Quark Matter '88,* proceedings of the Seventh International Conference on Ultrarelativistic Nucleus-Nucleus Collisions, Lenox, Massachusetts, 1988, edited by G. Baym, P. Braun-Munzinger, and S. Nagamiya [Nucl. Phys. **A498**, 227 (1989)].

[10]R. V. Gavai, J. Potvin, and S. Sanielevici, Phys. Rev. D **38**, 3266 (1988).

[11]M. Lüscher, Commun. Math. Phys. **85**, 39 (1982); P. Woit, Nucl. Phys. **B262**, 284 (1985); A. Phillips and D. Stone, Commun. Math. Phys. **103**, 599 (1986); G. Bhanot, F. Fucito, and S. Solomon, Phys. Lett. B **194**, 114 (1987); M. Göckeler, A. S. Kronfeld, M. L. Laursen, G. Schierholz, and U. J. Wiese, Nucl. Phys. **B292**, 349 (1987); J. Smit and J. C. Vink, Phys. Lett. B **194**, 433 (1987); J. C. Vink, *ibid.* **210**, 211 (1988); *ibid.* **212**, 483 (1988); D. J. R. Pugh and M. Teper, *ibid.* **218**, 326 (1989).

[12]M. I. Polikarpov and A. I. Veselov, Nucl. Phys. **B297**, 34 (1988).

[13]M. Campostrini, A. DiGiacomo, M. Maggiore, H. Panagopoulos, and E. Vicari, Nucl. Phys. **225B**, 403 (1989); M. Campostrini, A. DiGiacomo, M. Maggiore, S. Olejnik, H. Panagopoulos, and E. Vicari, in *Lattice '89,* proceedings of the International Symposium, Capri, Italy, 1989 [Nucl. Phys. B (Proc. Suppl.) (in press)].

[14]J. Hoek, M. Teper, and J. Waterhouse, Nucl. Phys. **B288**, 589 (1987); M. Teper, Phys. Lett. B **202**, 553 (1988).

[15]T. Hashimoto, S. Hioki, K. Hirose, T. Kanki, A. Kawazoe, M. Masujima, O. Myiamura, and Y. Osada, Osaka University Report No. OUAM 88-9-1, 1988 (unpublished).

[16]H. Gausterer, J. Potvin, S. Sanielevici, and P. Woit, Phys. Lett. B **209**, 439 (1989).

[17]T. Banks and A. Ukawa, Nucl. Phys. **B225** [FS9], 145 (1983); T. A. DeGrand and C. DeTar, *ibid.* **B225**, 590 (1983).

[18]T. P. Cheng and L. F. Li, *Gauge Theory of Particle Physics* (Oxford University Press, Oxford, England, 1984), Chap. 5.

[19]From phenomenological estimates it appears that the quenched value of $C(0)$ [obtained by setting $f_s = f_\pi$ in Eq. (3)] is numerically close to its real-world value (see Ref. 16).

[20]R. V. Gavai, J. Potvin, and S. Sanielevici, Phys. Rev. D **36**, 1912 (1987).

[21]R. V. Gavai, J. Potvin, and S. Sanielevici, Phys. Rev. D **40**, 2743 (1989).

[22]B. Berg, Phys. Lett. **104B**, 475 (1981); M. Lüscher, Nucl. Phys. **B200** [FS4], 61 (1982); D. Petcher and M. Lüscher, *ibid.* **B225** [FS9], 53 (1983).

[23]A. Ukawa, in *Lattice '89* (Ref. 13).